



Measurement of Masses and Widths of Excited Charm Mesons D_2^* and Evidence for Broad States

J. M. Link^a P. M. Yager^a J. C. Anjos^b I. Bediaga^b C. Göbel^b
A. A. Machado^b J. Magnin^b A. Massafferri^b
J. M. de Miranda^b I. M. Pepe^b E. Polycarpo^b A. C. dos Reis^b
S. Carrillo^c E. Casimiro^c E. Cuautle^c A. Sánchez-Hernández^c
C. Uribe^c F. Vázquez^c L. Agostino^d L. Cinquini^d
J. P. Cumalat^d B. O'Reilly^d I. Segoni^d M. Wahl^d J. N. Butler^e
H. W. K. Cheung^e G. Chiodini^e I. Gaines^e P. H. Garbincius^e
L. A. Garren^e E. Gottschalk^e P. H. Kasper^e A. E. Kreymer^e
R. Kutschke^e M. Wang^e L. Benussi^f M. Bertani^f S. Bianco^f
F. L. Fabbri^f A. Zallo^f M. Reyes^g C. Cawfield^h D. Y. Kim^h
A. Rahimi^h J. Wiss^h R. Gardnerⁱ A. Kryemadhiⁱ Y. S. Chung^j
J. S. Kang^j B. R. Ko^j J. W. Kwak^j K. B. Lee^j K. Cho^k
H. Park^k G. Alimonti^l S. Barberis^l M. Boschini^l A. Cerutti^l
P. D'Angelo^l M. DiCorato^l P. Dini^l L. Edera^l S. Erba^l
M. Giammarchi^l P. Inzani^l F. Leveraro^l S. Malvezzi^l
D. Menasce^l M. Mezzadri^l L. Moroni^l D. Pedrini^l
C. Pontoglio^l F. Prelz^l M. Rovere^l S. Sala^l
T. F. Davenport III^m V. Arenaⁿ G. Bocaⁿ G. Bonomiⁿ
G. Gianiniⁿ G. Liguoriⁿ M. M. Merloⁿ D. Panteaⁿ
D. Lopes Pegnaⁿ S. P. Rattiⁿ C. Riccardiⁿ P. Vituloⁿ
H. Hernandez^o A. M. Lopez^o E. Luiggi^o H. Mendez^o A. Paris^o
J. E. Ramirez^o Y. Zhang^o J. R. Wilson^p T. Handler^q
R. Mitchell^q D. Engh^r M. Hosack^r W. E. Johns^r M. Nehring^r
P. D. Sheldon^r K. Stenson^r E. W. Vaandering^r M. Webster^r
M. Sheaff^s

^aUniversity of California, Davis, CA 95616

^bCentro Brasileiro de Pesquisas Físicas, Rio de Janeiro, RJ, Brasil

^cCINVESTAV, 07000 México City, DF, Mexico

^d*University of Colorado, Boulder, CO 80309*

^e*Fermi National Accelerator Laboratory, Batavia, IL 60510*

^f*Laboratori Nazionali di Frascati dell'INFN, Frascati, Italy I-00044*

^g*University of Guanajuato, 37150 Leon, Guanajuato, Mexico*

^h*University of Illinois, Urbana-Champaign, IL 61801*

ⁱ*Indiana University, Bloomington, IN 47405*

^j*Korea University, Seoul, Korea 136-701*

^k*Kyungpook National University, Taegu, Korea 702-701*

^l*INFN and University of Milano, Milano, Italy*

^m*University of North Carolina, Asheville, NC 28804*

ⁿ*Dipartimento di Fisica Nucleare e Teorica and INFN, Pavia, Italy*

^o*University of Puerto Rico, Mayaguez, PR 00681*

^p*University of South Carolina, Columbia, SC 29208*

^q*University of Tennessee, Knoxville, TN 37996*

^r*Vanderbilt University, Nashville, TN 37235*

^s*University of Wisconsin, Madison, WI 53706*

See <http://www-focus.fnal.gov/authors.html> for additional author information

Abstract

Using data from the FOCUS experiment we analyze the $D^+\pi^-$ and $D^0\pi^+$ invariant mass distributions. We measure the D_2^{*0} mass $M_{D_2^{*0}} = (2464.5 \pm 1.1 \pm 1.9) \text{ MeV}/c^2$ and width $\Gamma_{D_2^{*0}} = (38.7 \pm 5.3 \pm 2.9) \text{ MeV}/c^2$, and the D_2^{*+} mass $M_{D_2^{*+}} = (2467.6 \pm 1.5 \pm 0.76) \text{ MeV}/c^2$ and width $\Gamma_{D_2^{*+}} = (34.1 \pm 6.5 \pm 4.2) \text{ MeV}/c^2$. We find evidence for broad structures over background in both the neutral and charged final state. If each is interpreted as evidence for a single $L = 1$, $j_q = 1/2$ excited charm meson resonance, the masses and widths are $M_{1/2}^0 = (2407 \pm 21 \pm 35) \text{ MeV}/c^2$, $\Gamma_{1/2}^0 = (240 \pm 55 \pm 59) \text{ MeV}/c^2$, and $M_{1/2}^+ = (2403 \pm 14 \pm 35) \text{ MeV}/c^2$, $\Gamma_{1/2}^+ = (283 \pm 24 \pm 34) \text{ MeV}/c^2$, respectively.

Interest in charm spectroscopy has shifted from the ground states of (0^- and 1^-) $c\bar{q}$ mesons to the orbitally and radially excited states. In the limit of infinitely heavy quark mass, the heavy-light meson behaves analogously to the hydrogen atom, *i.e.*, the heavier quark does not contribute to the orbital degrees of freedom (which are completely defined by the light quark). The angular momentum of the heavy quark is described by its spin S_Q , and that of the light degrees of freedom are described by $\mathbf{j}_q = \mathbf{s}_q + \mathbf{L}$, where s_q is the light quark spin and L is the orbital angular momentum of the light quark.

The quantum numbers S_Q and j_q are individually conserved. The quantum numbers of the excited $L = 1$ states are formed by combining \mathbf{S}_Q and \mathbf{j}_q . For $L = 1$ we have $j_q = 1/2$ and $j_q = 3/2$. When combined with S_Q they provide two $j_q = 1/2$ ($J=0,1$) states, and two $j_q = 3/2$ ($J=1,2$) states. In this paper these four states will be denoted by D_0^* , $D_1(j_q = 1/2)$, $D_1(j_q = 3/2)$ and D_2^* . Heavy Quark Symmetry (HQS) predicts the spectrum of excited charmed states [1]- [5]. In the HQS limit, conservation of both parity and j_q , requires that the strong decays $D_J^{(*)}(j_q = 3/2) \rightarrow D^{(*)}\pi$ proceed only via a D-wave while the decays $D_J^{(*)}(j_q = 1/2) \rightarrow D^{(*)}\pi$ proceed only via an S-wave. The states decaying to an S-wave are expected to be broad while those decaying in a D-wave are known to be narrow [6] [7]. Models predict that, when the heavy quark is the charmed quark, the physical states will have properties very close to those of the heavy quark limit. In the analysis described, we show the salient features of the $D^+\pi^-$ and $D^0\pi^+$ invariant mass distributions and measure parameters of the well-established narrow states. We observe an excess of events in the mass interval $2.25 \text{ GeV}/c^2$ to $2.40 \text{ GeV}/c^2$ that is consistent with a broad resonance and must be included in the representation of the data to produce a good fit.

The data for this paper were collected in the Wideband photoproduction experiment FOCUS during the Fermilab 1996–1997 fixed-target run. FOCUS [8] [9] [10] is an upgraded version of experiment E687 [11] [12]. In FOCUS, a forward multi-particle spectrometer is used to investigate the interactions of high energy photons on a segmented BeO target. We obtain a sample in excess of 1 million fully reconstructed charm particles in three decay modes: $D^0 \rightarrow K^-\pi^+$, $K^-\pi^+\pi^+\pi^-$ and $D^+ \rightarrow K^-\pi^+\pi^+$. (The charge-conjugate states are implicitly included throughout the paper.)

The FOCUS detector is a large aperture, fixed-target spectrometer with excellent vertexing and particle identification. A photon beam, with an endpoint energy of $\approx 300 \text{ GeV}$, is derived from the bremsstrahlung of secondary electrons and positrons. The charged particles which emerge from the target are tracked by two systems of silicon microvertex detectors. The upstream system [10], consisting of 4 planes (two views in 2 stations), is interleaved with the experimental targets, while the other system lies downstream of the target and consists of twelve planes of microstrips arranged in three views. These detectors provide high resolution separation of primary (production) and secondary (decay) vertices with an average proper time resolution of $\approx 30 \text{ fs}$ for 2-track vertices. The momentum of a charged particle is determined with five stations of multiwire proportional chambers by measuring deflections in two analysis magnets of opposite polarity. Three multicell threshold Čerenkov counters [8] are used to discriminate between electrons, pions, kaons, and protons.

1 Analysis Procedure and Results

The $L = 1$ charm mesons were reconstructed via $D^+\pi^-$ and $D^0\pi^+$ combinations. The D^0 decays were reconstructed in the channels $D^0 \rightarrow K^-\pi^+$ and $D^0 \rightarrow K^-\pi^+\pi^+\pi^-$. The D^+ decays were reconstructed in the channel $D^+ \rightarrow K^-\pi^+\pi^+$. To obtain a clean sample of high statistics charm decays, the vertexing and particle identification cuts were optimized separately for each decay mode. The significance of separation between the production and decay vertex, ℓ/σ_ℓ (where ℓ is the separation between the primary and secondary vertex, and σ_ℓ is its error), was required to be greater than 5, 10, and 12 respectively for the three decay modes. The interaction vertex was formed from the D candidate, the bachelor pion and at least one additional charged track [11] and was required to be located within the target material. The pion and kaon candidates were required to have a Čerenkov identification consistent with the selected particle hypothesis. Further, we required that the decay $D^0 \rightarrow K^-\pi^+\pi^+\pi^-$ be reconstructed outside of target material and that $|\cos\theta_K| < 0.7$ for the $D^0 \rightarrow K^-\pi^+$ decay, where θ_K is defined as the angle between the D lab frame momentum and the kaon momentum in the D center of mass frame. Our starting samples for the decay modes with the above cuts are 210,000, 125,000 and 200,000 events respectively (see Figure 1 a-c). Combinations within $\pm 2\sigma$ of the nominal masses were retained as D candidates. Events with D^0 candidates coming from D^{*+} decays were eliminated by applying a $\pm 3\sigma$ cut around the $D^{*+} - D^0$ mass difference (see Figure 1 d).

Figure 2a) shows the distribution of the invariant mass difference

$$\Delta M_0 \equiv M((K^-\pi^+\pi^+)\pi^-) - M(K^-\pi^+\pi^+) + M_{\text{PDG}}(D^+) \quad (1)$$

where $M_{\text{PDG}}(D^+)$ is the world average D^+ mass [7]. Figure 2a) shows a pronounced, narrow peak near a mass $M \approx 2460 \text{ MeV}/c^2$, which is consistent with the D_2^{*0} mass. The additional enhancement at $M \approx 2300 \text{ MeV}/c^2$ is consistent with feed-downs from the states D_1^0 and D_2^{*0} decaying to $D^{*+}\pi^-$ when the D^{*+} subsequently decays to a D^+ and undetected neutrals.

The mass difference

$$\Delta M_+ \equiv M((K^-\pi^+, K^-\pi^+\pi^-\pi^+)\pi^+) - M(K^-\pi^+, K^-\pi^+\pi^-\pi^+) + M_{\text{PDG}}(D^0) \quad (2)$$

spectrum (Figure 2b) shows similar structures to the ΔM_0 spectrum. The prominent peak is consistent with a D_2^{*+} of mass $M \approx 2460 \text{ MeV}/c^2$. The additional enhancement at $M \approx 2300 \text{ MeV}/c^2$ is again consistent with feed-downs.

We fit the invariant mass difference histograms with terms for the D_2^{*0} , D_2^{*+} peaks, D_1 and D_2^* feed-downs, combinatoric background and the possibility of a broad resonance. Fit terms were independent for each histogram except for specific systematic tests, and all fit parameters were allowed to float except in tests which are described below.

The D_2^{*0} , D_2^{*+} signals were represented with relativistic D-wave Breit-Wigner functions convoluted with a Gaussian resolution function ($\sigma = 7 \text{ MeV}/c^2$). The σ of the resolution function was determined by processing PYTHIA [13] events through the FOCUS detector simulation and reconstruction codes.

The combinatoric background was represented by a continuum function discussed below. The feed-downs were represented using line shapes determined by reconstructing simulated $D^*\pi$ events as $D\pi$. The masses and widths used for the $D^*\pi$ and $D\pi$ came from the PDG or from our fit to the D_2^* as described below. Only the amplitudes of the feed-downs were allowed to float in the fit. A relativistic S-wave Breit-Wigner function was used to represent a broad resonance contribution (motivated below).

In order to determine functions for the combinatoric background, several studies were performed. We studied the distribution of events in wrong sign combinations (the $D^{*+}(D^0\pi^+)\pi^-$ reflection from the D_1 is very small), simulations where no $L = 1$ charm mesons are present, and data sidebands of the D^+ and D^0 . We found that in all these cases, the combinatoric background is well described by a single exponential beyond $2250 \text{ MeV}/c^2$. Several functions with threshold characteristics (described in Section 2) were utilized to include information below $2250 \text{ MeV}/c^2$. Our final result is based on a function adapted from an E687 analysis [14] of excited D states

$$\exp(A + Bx)(x - C)^D \tag{3}$$

where $x \equiv \Delta M_{0,+}$, and A, B, C and D are free parameters in the fit. (Care is required to limit the range of the C parameter so that the threshold term does not become imaginary.) With this function representing combinatoric background, we produced final results that were stable with consistently good confidence levels over a variety of fit ranges. No combinatoric shapes consistent with our background studies were able to describe either signal histogram unless we included a function representing a broad resonance.

In order to illustrate the motivation for including the broad resonance, we show two representative fits performed without the broad resonance. The distributions shown were fit with the D_2^{*0} , D_2^{*+} parameters fixed to the world average values [7] (Figure 2 a,b), and with the D_2^{*0} , D_2^{*+} parameters allowed to freely float (Figure 2 c,d). Individual fit components, and an expanded view of the region around $2400 \text{ MeV}/c^2$ are shown in the figure. In both cases, the

fit quality is unacceptable, even when the D_2^* parameters float to values far from the PDG values. Both fits indicate an excess of events between the D_2^* signal and the feed-downs. We expect the background to be well described by a single exponential in this region, but the fit is unable to simultaneously describe the data at masses higher than the D_2^* peak and at masses lower than the D_2^* peak. Since the behavior of the combinatoric background is heavily influenced by the events with invariant mass difference higher than the D_2^* peak, departures from the exponential form near $2400 \text{ MeV}/c^2$ become evident.

While we are unable to rule out the possibility that the excess is due to feed-down from higher mass charm states, we chose to describe the excess with an S-wave relativistic Breit-Wigner function centered roughly near the excess.

In Figure 3 a-b) we show a fit to the data between $2120 \text{ MeV}/c^2$ and $5000 \text{ MeV}/c^2$ that includes an S-wave relativistic Breit-Wigner in addition to previously described terms. Agreement is excellent with a fit confidence level of 22%. For self consistency, the D_2^* parameters measured in this fit are used to recompute the feed-down lineshape. When the histograms were refit using the new feed-down lineshape, the fit confidence level increased to 28% without a significant change in the returned fit parameters. The results of this last fit are shown in Table 1 together with PDG values where available.

We find that the mass and width returned by the fit are increased compared to those reported by the PDG. Further, the yields and returned errors for the broad states indicate a significant excess is present.

Although we are unable to distinguish between a broad state produced directly via a D_0^* and the feed-down from a broad D_1 state, we can make some qualitative comparisons. If the ratio of D_1 to D_2^* production is the same for the charged and neutral modes, and the decays of these states are dominated by $D\pi$ and/or $D^*\pi$, a meaningful comparison between the relative abundance of the feed-downs and the broad resonance to the D_2^* signal can be made. With these assumptions, one expects that the feed-down from the D_2^* and D_1 narrow states to be larger relative to the D_2^* peak for $D^0\pi^+$ modes since the D^{*0} has no D^+ channel. This is what we observe. We also find that the broad state contribution in the $D^0\pi^+$ mode relative to the D_2^{*+} peak is larger than the broad state contribution in the $D^+\pi^-$ relative to the D_2^{*0} peak. This suggests some feed-down contribution to the broad state, perhaps from a broad D_1 state (the search for a $D^*\pi$ broad resonance is being performed and will be included in a later publication on $D^*\pi$ states).

Further, the fit parameters representing the broad S-wave state are statistically indistinguishable for both charged and neutral states. This is expected for broad states differing only by the flavor of the light quark and dominated by decay into a $D^{(*)}$ meson and a pion.

2 Systematic Checks

Our systematic studies included a verification of the fit, fits using different functional forms for the background, different shapes for the feed-down, fits excluding the feed-down regions, fits over different regions of the data histogram, a fit where we shifted our bin centers, a fit with the bin size reduced by a factor of 2, fits in which we excluded data where the background shape is expected to differ from that of Equation 3, and separate fits for particle and anti-particle distributions. All the contributions were added in quadrature (see Table 2) and are described in more detail below.

The fitting algorithm was extensively tested by fluctuating the data histogram, comparing errors returned by the fit and the spread of parameters from repeated trials. We have also performed repeated fits to histograms generated with the fit function. We observe that the goodness of fit is acceptable, that the central values are unbiased and that the errors correctly describe the variation of the central values over the trials.

We split the sample into particle and anti-particle, producing two statistically separate data samples. These two samples were fit, and additional error (if any) was assessed until the parameters returned by the fit agreed with their average

$$\sum(x - x_{\text{avg}})^2 = \sigma_{\text{stat}}^2 + \sigma_{\text{extra}}^2 \quad (4)$$

The deviations in the fit parameters returned by the tests described below were added in quadrature to the split sample estimate to assess a total systematic error.

In addition to the modified E687 function, we fit the data with a pure exponential background function

$$\exp(A + Bx) \quad (5)$$

We also fit the data with a background function including a Gaussian term

$$\exp(A + Bx + Cx^2) \quad (6)$$

and we fit the data with a background function that was used by L3 [15]

$$\exp(A + Bx)/(1 + \exp(D - x)/E) \quad (7)$$

We used feed-down functions based on PDG values for the D_2^* parameters.

Table 1

Measured masses and widths for narrow and broad structures in $D^+\pi^-$ and $D^0\pi^+$ invariant mass spectra. The first error listed is statistical and the second is systematic. Units for the masses and widths are MeV/c^2 .

	D_2^{*0}	D_2^{*+}	$D_2^{*+} - D_2^{*0}$	$D_{1/2}^0$	$D_{1/2}^+$
Yield	$5776 \pm 869 \pm 696$	$3474 \pm 670 \pm 656$		9810 ± 2657	18754 ± 2189
Mass	$2464.5 \pm 1.1 \pm 1.9$	$2467.6 \pm 1.5 \pm 0.76$	$3.1 \pm 1.9 \pm 0.9$	$2407 \pm 21 \pm 35$	$2403 \pm 14 \pm 35$
PDG03	2458.9 ± 2.0	2459 ± 4	0 ± 3.3		
Width	$38.7 \pm 5.3 \pm 2.9$	$34.1 \pm 6.5 \pm 4.2$		$240 \pm 55 \pm 59$	$283 \pm 24 \pm 34$
PDG03	23 ± 5	25_{-7}^{+8}			

In addition we used feed-down functions based on our measured values for the D_2^* parameters. We also fit the entire histogram from $2030 \text{ MeV}/c^2$ to $5000 \text{ MeV}/c^2$ while excluding the feed-down region ($2230 \text{ MeV}/c^2 - 2400 \text{ MeV}/c^2$) with both the E687 modified function and the L3 function, and we performed an additional fit with the E687 modified function where we exclude the region between $2120 \text{ MeV}/c^2$ and $2190 \text{ MeV}/c^2$ in addition to excluding the feed-down regions.

We find that the data samples at very high (> 30) ℓ/σ_ℓ and high D momentum ($P_D > 70 \text{ GeV}/c$) have a significantly different background distribution. We test the effect on our final result by removing these samples and by refitting.

In order to determine the systematic uncertainty in our mass difference due to the mass scale of the FOCUS spectrometer, we measured the mass differences $M(D^*) - M(D)$ and $M(\psi(2S)) - M(J/\psi)$. The quoted uncertainty is the additional contribution (added in quadrature to the statistical error) needed for our measurements to be in agreement with world average values.

The contributions to the final systematic errors shown in Table 1 are listed in Table 2. The yields for both the narrow and broad states show a large variation depending on the fit considered. This is due to the wide range of background shapes investigated. Further, since the broad resonance is not fully contained in the fits, determination of the yield of the broad resonance depends on how much of the data histogram is included in the fit, and quoting a systematic error on this yield becomes problematic. Rather than quote a systematic error on the yield of the broad state, we looked at the statistical significance, $\text{Yield}/\delta(\text{Yield})$, for each fit considered. In Figure 4 we show that the statistical significance of our quoted result is a good representation of the fits tried.

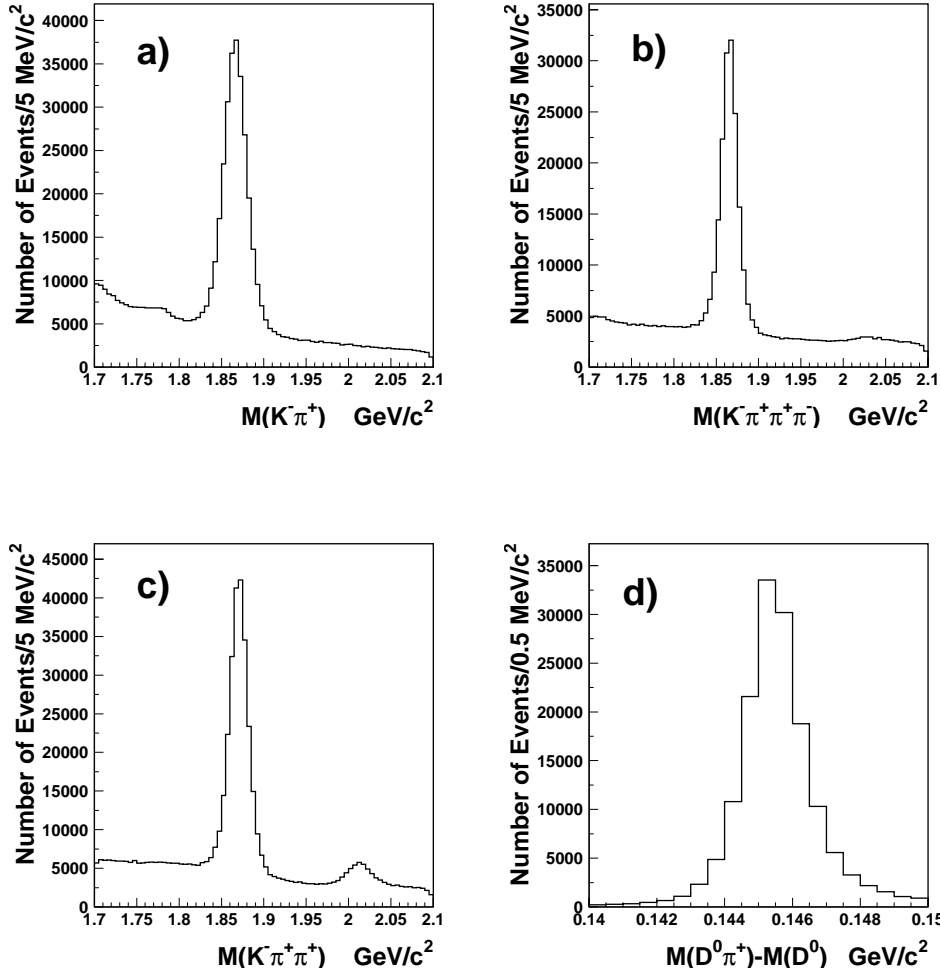


Fig. 1. Invariant mass plots for: a) $D^0 \rightarrow K^-\pi^+$; b) $D^0 \rightarrow K^-\pi^+\pi^+\pi^-$; c) $D^+ \rightarrow K^-\pi^+\pi^+$. Invariant mass difference plot for d) $D^{*+} \rightarrow D^0\pi^+$.

Table 2

Individual contributions to the systematic error. Units are MeV/c^2

	D_2^{*0}	D_2^{*0}	D_2^{*+}	D_2^{*+}	$D_{1/2}^0$	$D_{1/2}^0$	$D_{1/2}^+$	$D_{1/2}^+$	$D_2^{*+} - D_2^{*0}$
	Mass	Width	Mass	Width	Mass	Width	Mass	Width	Mass
$\ell/\sigma < 30$	0.160	1.231	0.134	0.960	0.926	15.73	0.050	2.871	0.294
Part/Antipart	1.67	0	0.53	0	0	0	0	31.4	0
$P_D < 70\text{GeV}/c$	0.227	0.705	0.392	1.983	2.482	8.509	10.38	2.500	0.165
Different Fits	0.412	0.272	0.124	0.693	10.48	43.95	1.439	8.635	0.353
Fit Regions	0.376	0.536	0.174	0.991	1.571	12.80	1.209	6.657	0.315
Feed-down tests	0.633	2.373	0.262	3.289	32.71	31.91	32.45	6.137	0.443
Binning tests	0.442	0.576	0.113	0.770	6.584	6.652	6.380	0.894	0.550
Mass Scale	0.100	0	0.100	0	0.100	0	0.100	0	0.100
Total syst. error	1.94	2.89	0.76	4.2	35.1	59.0	34.7	34.0	0.91

Table 3

Predicted mass differences with respect to the D meson compared to this result. The charged and neutral states are averaged. In the case of the broad state we compare our result to D_0^* only. Units are MeV/c^2 .

Reference	D_2^*	D_1	D_1	D_0^*
	$j_q = 3/2$ 3P_2	$j_q = 3/2$ 3P_1	$j_q = 1/2$ 1P_1	$j_q = 1/2$ 3P_0
This paper	599			538
World Av. [7]	593	556		
Kalashnikova et al. (2002) [24]	579	562	603	564
Di Pierro et al. (2001) [23]	592	549	622	509
Ebert et al. (1998) [22]	584	539	626	563
Isgur (1998) [21]	594	549	719	699
Godfrey and Kokoski (1991) [3]	620	590	580	520
Godfrey and Isgur (1985) [2]	620	610	560	520
Eichten et al. (1980) [20]	645	637	498	489
Barbieri et al. (1976) [19]	428	380	339	259
De Rujula et al. (1976) [18]	494	464	384	374

3 Conclusions

FOCUS has measured the $D^+\pi^-$ and $D^0\pi^+$ mass spectra and provided new values for the masses and widths of the D_2^{*0} and D_2^{*+} mesons (Table 1) with errors less than or equal to the errors on world averages.

The D_2^* masses and widths measured are found to be higher than the world averages. We attribute the change to the inclusion of an underlying broad state.

We find significant evidence for a broad excess which we parameterize with an S-wave resonance. Our results are consistent with a broad resonance occurring near $2400 \text{ MeV}/c^2$ with a width of about $250 \text{ MeV}/c^2$ in both the charged and neutral modes. We are unable to distinguish whether the broad excess is due to a state such as the D_0^* , predicted by HQS at $M \approx 2400$ and width $\approx 100 - 200 \text{ MeV}/c^2$, or due to feed-down from another broad state, such as the $D_1(j_q = 1/2)$, or whether both states contribute.

Evidence for $L = 1$ broad (S-wave) states has been previously presented in B decays by CLEO in the $D^{*+}\pi^-$ final state [16], and BELLE [17] in the $D^{*+}\pi^-, D^+\pi^-$ final states.

Our measurements are compared to theory predictions in Table 3. The D_2^* masses are in good agreement with [21] and [23]. Reference [23], in addition, predicts a $D_2^*-D_0^*$ mass shift consistent with our evidence, while [21] predicts a shift with the opposite sign.

We would like to thank the staffs of Fermi National Accelerator Laboratory, INFN of Italy, and the physics departments of the collaborating institutions for their assistance. This research was partly supported by the U. S. Department of Energy, the U. S. National Science Foundation, the Italian Istituto Nazionale di Fisica Nucleare and Ministero dell'Istruzione, dell'Università e della Ricerca, the Brazilian Conselho Nacional de Desenvolvimento Científico e Tecnológico, CONACyT-México, the Korean Ministry of Education, and the Korean Science and Engineering Foundation.

References

- [1] E. V. Shuryak, Nucl. Phys. B **198**, 83 (1982).
- [2] S. Godfrey and N. Isgur, Phys. Rev. D **32**, 189 (1985).
- [3] S. Godfrey and R. Kokoski, Phys. Rev. D **43**, 1679 (1991).
- [4] N. Isgur and M.B. Wise, Phys. Rev. Lett. **66**, 1130 (1991).
- [5] E. J. Eichten, C. T. Hill and C. Quigg, Phys. Rev. Lett. **71**, 4116 (1993).
- [6] J. Bartelt and S. Shukla, Annu. Rev. Nucl. Part. Sci 1995 **45** 133-61; F. L. Fabbri, "Heavy flavor spectroscopy," Frascati Phys. Ser. **15** (1999) 627-639; S. Bianco, F. L. Fabbri, D. Benson and I. Bigi, "A cicerone for the physics of charm," arXiv:hep-ex/0309021 (to appear on Rivista del Nuovo Cimento).
- [7] K. Hagiwara *et al.*, Phys. Rev. **D66**, 010001 (2002).
- [8] J. M. Link *et al.* [FOCUS Collaboration], Nucl. Instrum. Meth. A **484** (2002) 270.
- [9] J. M. Link *et al.* [FOCUS Collaboration], Nucl. Instrum. Meth. A **484** (2002) 174.
- [10] J. M. Link *et al.* [FOCUS Collaboration], Nucl. Instrum. Meth. A **516** (2003) 364.
- [11] P. L. Frabetti *et al.* (E687 Coll.), Nucl. Instrum. Meth. **A320**, 519 (1992).
- [12] P. L. Frabetti *et al.*, Nucl. Instrum. Meth. A **329** (1993) 62.
- [13] T. Sjostrand, L. Lonnblad, S. Mrenna and P. Skands, arXiv:hep-ph/0308153.
- [14] P. L. Frabetti *et al.* [E687 Collaboration], Phys. Rev. Lett. **72**, 324 (1994).
- [15] M. Acciarri *et al.* [L3 Collaboration], Phys. Lett. B **453**, 73 (1999).
- [16] S. Anderson *et al.* (CLEO Collaboration), Conference report CLEO CONF 99-6 (1999).
- [17] K. Abe *et al.* [Belle Collaboration], arXiv:hep-ex/0307021.

- [18] A. De Rujula, H. Georgi and S. L. Glashow, Phys. Rev. Lett. **37**, 785 (1976).
- [19] R. Barbieri, R. Kogerler, Z. Kunszt and R. Gatto, Nucl. Phys. B **105**, 125 (1976).
- [20] E. Eichten, K. Gottfried, T. Kinoshita, K. D. Lane and T. M. Yan, Phys. Rev. D **21**, 203 (1980).
- [21] N. Isgur, Phys. Rev. D **57**, 4041 (1998).
- [22] D. Ebert, V. O. Galkin and R. N. Faustov, Phys. Rev. D **57**, 5663 (1998) [Erratum-ibid. D **59**, 019902 (1999)] [arXiv:hep-ph/9712318]; D. Ebert, R. N. Faustov and V. O. Galkin, arXiv:hep-ph/0110190.
- [23] M. Di Pierro and E. Eichten, Phys. Rev. D **64**, 114004 (2001)
- [24] Y. S. Kalashnikova and A. V. Nefediev, Phys. Lett. B **530**, 117 (2002) [arXiv:hep-ph/0112330].

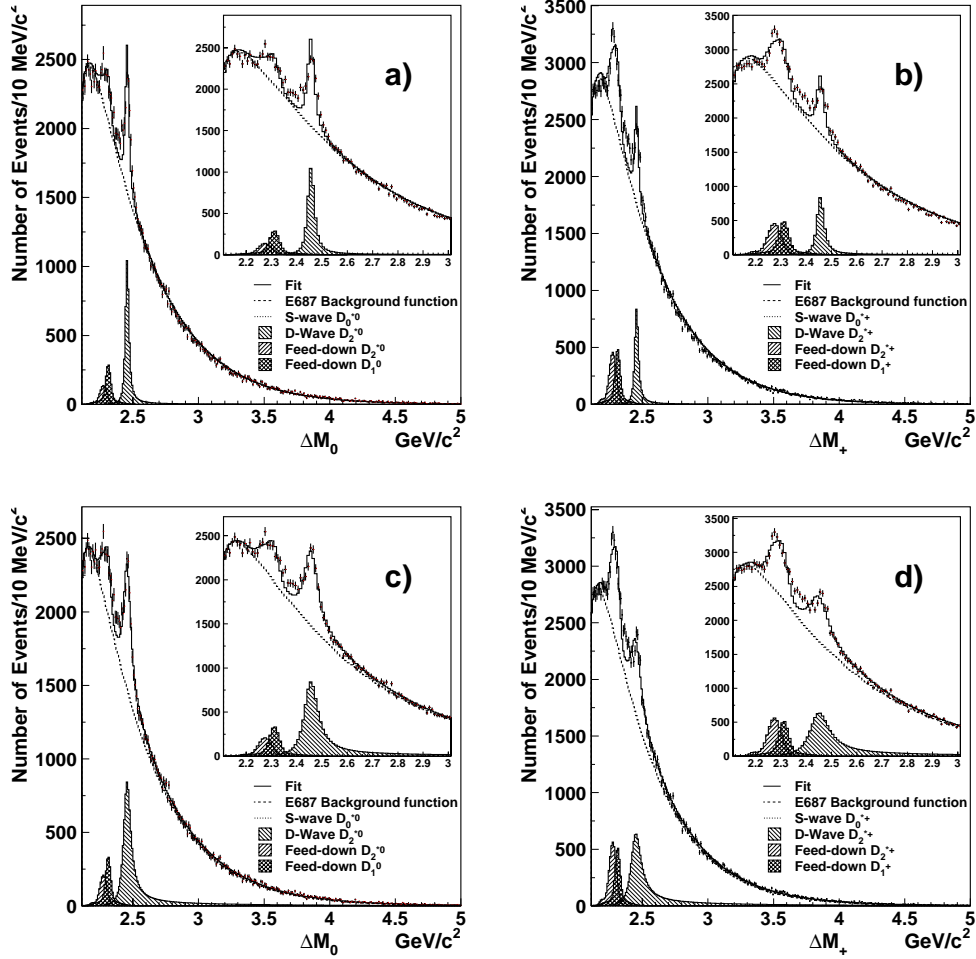


Fig. 2. The fit to the $D^+\pi^-$ and $D^0\pi^+$ mass spectra for the case where the D-wave mass and width are fixed to the PDG values, the background is described by Equation 3, and no broad resonance is included, is shown in a) and b). The case where the D-wave mass and width are allowed to float in the fit is shown in c) and d). Note that the none of these fits provides a good description of the data between the feed-downs ($\sim 2300 \text{ MeV}/c^2$) and the D_2^* peak ($\sim 2500 \text{ MeV}/c^2$). In Figure 3, we show that the data are well described when a broad resonance is included in the fit.

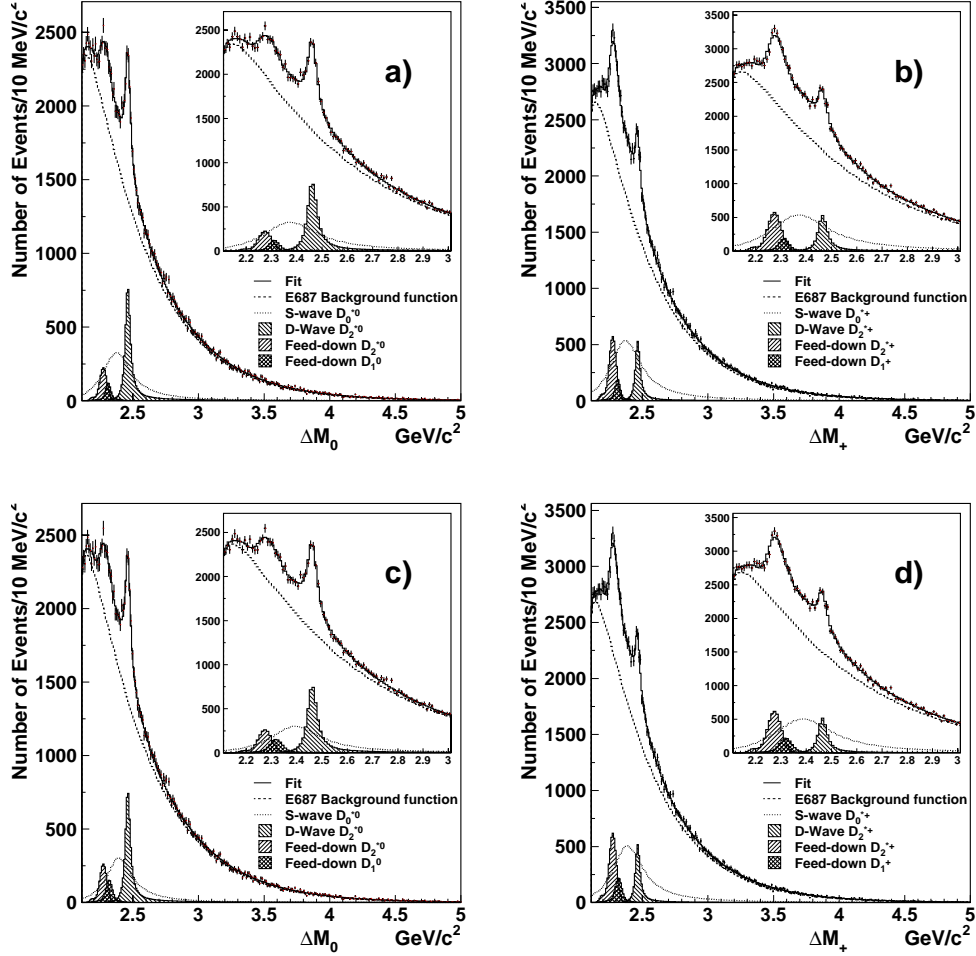


Fig. 3. The fit to the $D^+\pi^-$ and $D^0\pi^+$ mass spectra including a term for an S-wave resonance. The case with the mass and width for the $D_1(3/2)$ and D_2^* feed-downs fixed to the PDG values is shown in a) and b). The case with the mass and width for the $D_1(3/2)$ feed-down fixed to the PDG values and for the D_2^* feed-down determined by fits in a) and b) is shown in c) and d). Notice the excellent agreement when the broad resonance is included (described in more detail in the text).

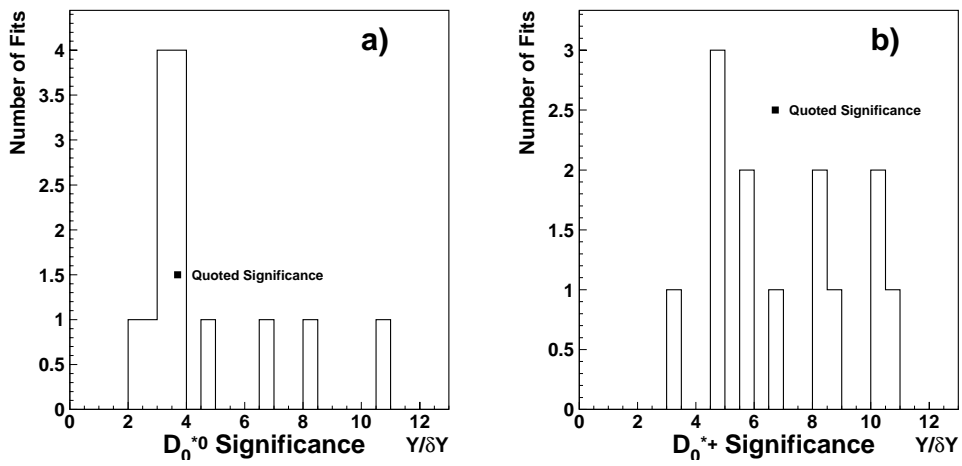


Fig. 4. Statistical significance of broad states signals in the $D^+\pi^-$ (a) and $D^0\pi^+$ (b) channels for various fits.